

# Microfluidic artificial photosynthetic system for continuous NADH regeneration and L-glutamate synthesis

Huichao Lin,<sup>†a</sup> Yang Liu,<sup>†a</sup> Chonghui Yang,<sup>a</sup> Gaozhen Zhao,<sup>a</sup> Jiaao Song,<sup>a</sup> Taiyi Zhang,<sup>a</sup> and Xiaowen Huang<sup>\*a</sup>

<sup>a</sup>. State Key Laboratory of Biobased Material and Green Papermaking, Department of Bioengineering, Qilu University of Technology (Shandong Academy of Sciences), Jinan, China, 250300.

## Supplementary Information

1. Calibration of protein amount
2. HPLC analysis
3. Characterization of the few-layer g-C<sub>3</sub>N<sub>4</sub>
4. Optical microscope analysis
5. SEM images of GIMR microchannels before and after the reaction

## 1. Calibration of protein amount

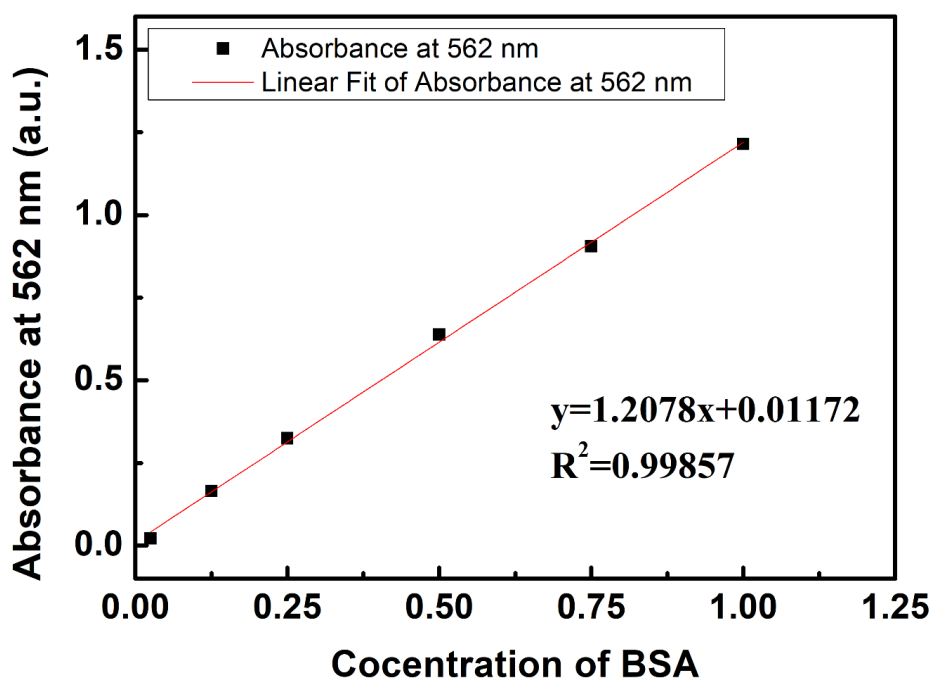


**Figure S1. Calibration of protein amount determined from BSA solution.** Protein amount was qualified using the BCA Protein Assay Kit (Meilune Biotech, China), which were determined by measuring the absorbance at the wavelength of 562 nm using a Ultramicro ultraviolet spectrophotometer (NanoDrop 2000, Thermo Fisher Scientific, USA). BSA solution ( $0.025-1 \text{ mg}\cdot\text{mL}^{-1}$ ) were selected as standards to plot the calibration curve.

## 2. HPLC analysis

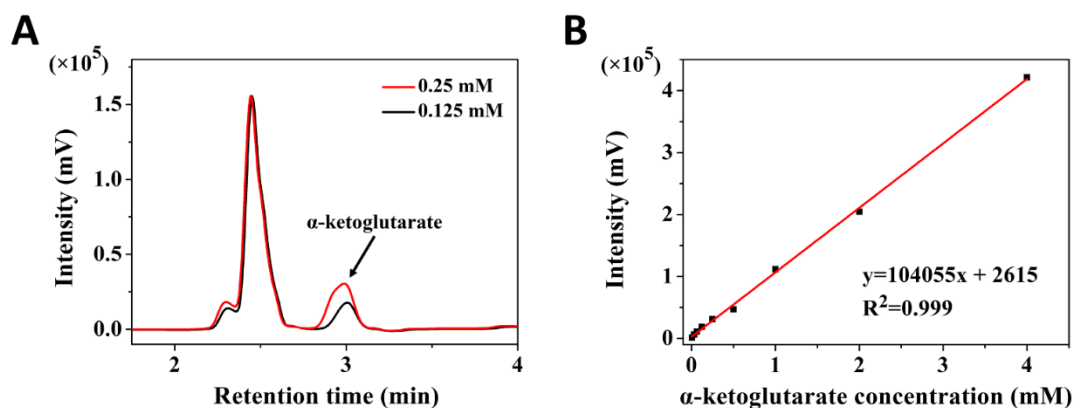


**Figure S2. HPLC chromatogram and standard curve of  $\alpha$ -ketoglutarate.** (A) HPLC chromatography of the  $\alpha$ -ketoglutarate with the concentration of 0.25 mM and 0.125 mM. (B) Calibration of the height of the  $\alpha$ -ketoglutarate as a function of its concentration. The monitoring of the reaction was performed using a high-performance Liquid Chromatography (HPLC, LC-20AB, Shimadzu Corporation). A C18 column (Acchrom Tech, 4.6 mm $\times$ 250 mm, 5  $\mu$ m) was used for the chromatography separation. The samples were eluted with phosphoric acid (0.01%) at the flow rate of 1.0 mL min $^{-1}$  and detected at 203 nm.

### 3. Characterization of the few-layer g-C<sub>3</sub>N<sub>4</sub>

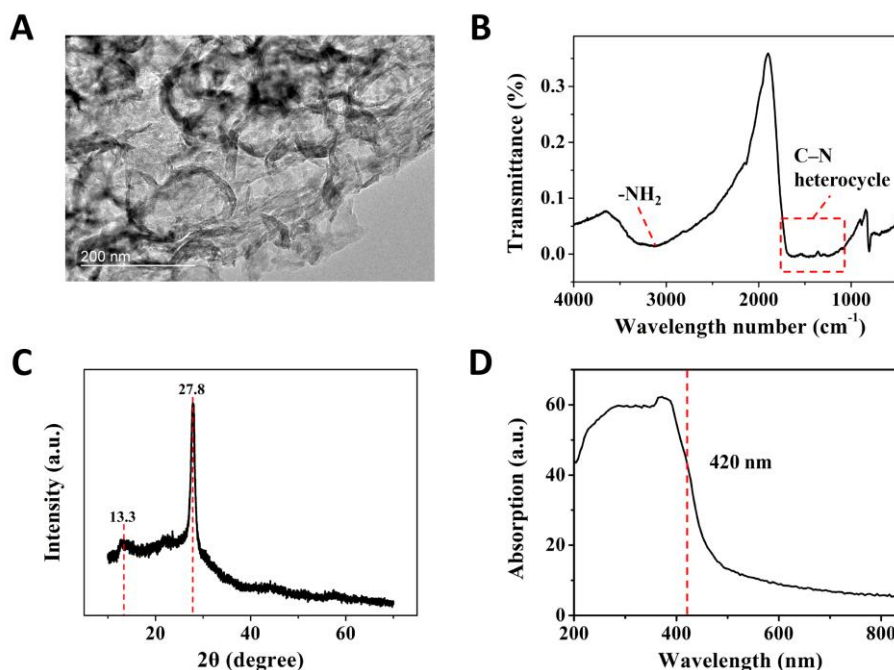


**Figure S3. Characterization of the few-layer g-C<sub>3</sub>N<sub>4</sub>.** (A) The TEM image of the few-layer g-C<sub>3</sub>N<sub>4</sub> material, shows the graphene-like appearance. (B) FTIR spectrum of the few-layer g-C<sub>3</sub>N<sub>4</sub>, showing typical C–N heterocycle stretches at 1600-1200 cm<sup>-1</sup>, as well as the characteristic breathing mode of triazine units at 806 cm<sup>-1</sup>. The broad peaks between 3000 and 3500 cm<sup>-1</sup> are attributed to the N–H band. (C) XRD spectrum of the few-layer g-C<sub>3</sub>N<sub>4</sub> with two peaks at 13.3° and 27.8°, ascribed to the lattice planes parallel to the c-axis and the stacking of the conjugated aromatic system, respectively. (D) UV-vis absorption spectrum of the few-layer g-C<sub>3</sub>N<sub>4</sub>, which is broad, ranging from UV light to visible light.

#### 4. Optical microscope analysis

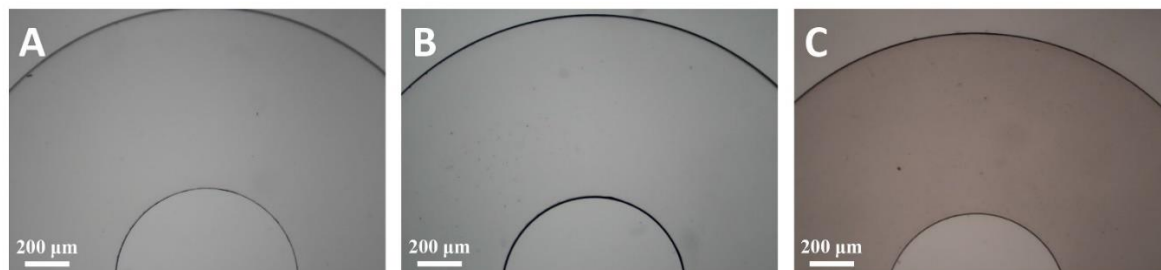


**Figure S4. Optical microscopic images of microchannels after each step of the immobilization procedures.** (A) Blank PDMS microchannel, which is transparent. (B) APTES-modified microchannel, which is still transparent, but uniform coating thickness is observed on the channel wall. (C) PDA-modified microchannels, which become opaque and brown. The scale bar is 200  $\mu\text{m}$ .

#### 5. SEM images of GIMR microchannels before and after the reaction

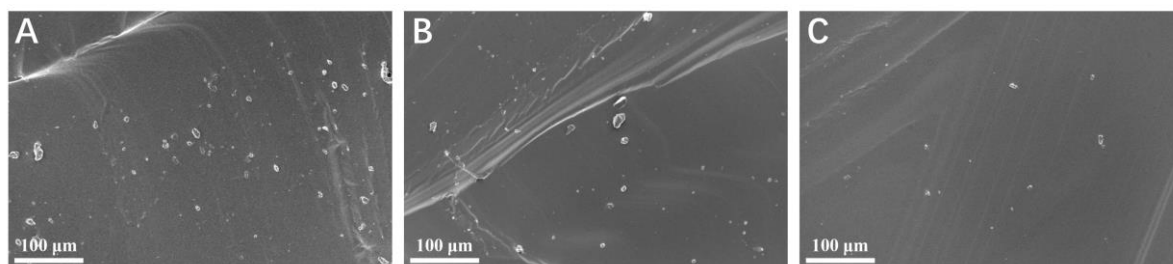


**Figure S5. SEM images of GIMR microchannels before and after the reaction.** (A) Before the reaction. (B) After the one reaction. (C) After the ten reactions. The number of blocks after the reaction decreased gradually. The scale bar is 100  $\mu\text{m}$ .